ELSEVIER

Journal of Alloys and Compounds 275–277 (1998) 214–218

Journal of ALLOYS AND COMPOUNDS

Spectroscopic properties of rare earths in $K_5Bi_{1-x}(RE)_x(MoO_4)_4$ crystals

M. Voda, R. Balda, I. Sáez de Ocáriz, L.M. Lacha, M.A. Illarramendi, J. Fernández*

Applied Physics Department I, ETSII y Telecom., Alameda Urquijo s/n 48013, Bilbao, Spain

Abstract

The luminescence of the RE=Pr^{3+}, Eu^{3+}, Nd^{3+} ions in $K_5Bi_{1-x}(RE)_x(MoO_4)_4$ ($x \leq 1$) crystals has been investigated by using steady-state and time-resolved laser spectroscopy. The Pr^{3+} emission in these crystals, at low dopant concentrations, are characterized by an intense $^1D_2 \rightarrow {}^3H_4$ red luminescence. Under excitation in the $^3P_0$ state the crystals show emission from both $^3P_0$ and $^1D_2$ levels. At Pr^{3+} concentrations higher than $x=0.005$, even at 4.2 K, the $^1D_2$ level shows a strong concentration quenching. Site-selective spectroscopy of the $^3P_0$ level exhibits remarkable site effects. Resonant fluorescence line narrowing spectroscopy of the $^5D_0$ level of Eu^{3+} shows the existence of two main broad crystal field site distributions for the europium ion, together with two other minor distinguishable sites. Referring to Nd^{3+}, the time-resolved $^4F_{3/2} \rightarrow {}^4I_{9/2}$ emission spectra obtained by exciting in the $^4G_{5/2}$ level show features which may suggest the presence of more than one Nd^{3+} site. © 1998 Elsevier Science S.A.

Keywords: Luminescence; Time-resolved laser spectroscopy; Pr^{3+}; Crystal field; Nd^{3+}

1. Introduction

Palmierite-type $K_5R(MoO_4)_4$ (R=Bi, Y, rare earth) compounds are of great interest as potential stoichiometric laser materials [1,2]. The combination of high concentration and small quenching allows miniaturization of the laser which is interesting for laser applications in integrated optics. The optical and laser properties of Nd^{3+} ions have been reported for $K_5Nd(MoO_4)_4$ and $K_5Bi_{1-x}Nd_x(MoO_4)_4$ crystals by Kaminskii et al. [1]. The spectroscopic properties of $K_5Eu(MoO_4)_4$ have been reported by Huber et al. [3].

In the present work we investigate the spectroscopic properties of RE=Pr^{3+}, Eu^{3+}, Nd^{3+} ions in $K_5Bi_{1-x}(RE)_x(MoO_4)_4$ ($x \leq 1$). The study includes absorption, steady-state emission, lifetimes, and site-selective time-resolved laser spectroscopy, and fluorescence quenching processes. This study demonstrates the existence of more than one distinguishable site distribution for RE in these compounds.

2. Experimental

Solid solutions of the $K_5Bi_{1-x}(RE)_x(MoO_4)_4$, RE=$Pr^{3+}$, Eu^{3+}, Nd^{3+} were formed within the K_2O–Bi_2O_3–$(RE)_2O_3$–MoO_3 system and high optical quality single crystals were grown in our laboratory by the Czochralski technique in the whole concentration region of $x=0,..1$. All crystals were grown under ambient atmosphere in a platinum crucible by pulling them perpendicularly to the *c*-direction. The crystal structures of $K_5(RE)(MoO_4)_4$ [4] and $K_5Bi(MoO_4)_4$ [2] were found to be isomorphous with the structure type of palmierite $K_2Pb(SO_4)_2$. The corresponding crystallochemical formula should therefore be written as $\{K\}_2[K_{0.5}(RE)_{0.5}](MoO_4)_2$. These compounds crystallize in the trigonal system, class $\bar{3}m$, space group R3m. The solid solutions $K_5Bi_{1-x}(RE)_x(MoO_4)_4$ present the same palmierite-type structure which is characterized by double layers of $(MoO_4)_4$ tetrahedra perpendicular to the *c*-axis bonded by $\{K^+\}$ ions arranged between the layers. The remaining K^+ and $(RE)^{3+}$ (or Bi^{3+}) ions, according to their contribution $[K_{0.5}(RE,Bi)_{0.5}]$, are randomly distributed on a plane hexagonal network, embedded within the $(MoO_4)_4$ double layers.

The sample temperature was varied between 4.2 and 300 K with a continuous flow cryostat. Conventional absorption spectra were performed with a Cary 5 spectrophotometer. The steady-state emission measurements were made with an argon laser as exciting light. Lifetime measurements were performed with a pulsed tunable dye laser operated with Coumarine 480 pumped by a frequency doubled Nd:YAG laser of 9 ns pulse width and 0.08 cm^{-1} linewidth. Data were processed by a EGG-PAR boxcar integrator. The time-resolved fluorescence was analyzed

---

*Corresponding author. Fax: +34 4 4414041; e-mail: wupferoj@bicc00.bi.ehu.es

0925-8388/98/$19.00
PII: S0925-8388(98)00306-5

and detected by an EGG-PAR Optical Multichannel Analyzer.

3. Results

3.1. Spectroscopic properties of Pr^{3+}

Conventional polarized room-temperature absorption spectra were obtained for all samples ($x=0.005$, 0.01, 0.03, 0.05, and 0.1), in the 400–2500 nm range, with a Cary 5 spectrophotometer. The spectra consist of several bands corresponding to transitions between the $^3H_4$ ground state and the excited multiplets belonging to the $4f^2$ configuration of the praseodymium ion.

The room temperature steady-state emission spectra were obtained for all concentrations in the 470–800 nm spectral range by exciting with an argon laser. In order to compare the emission of crystals with a different Pr^{3+} concentration, emission measurements were performed in such a way that an absolute comparison could be made among different samples [5]. Fig. 1 shows the σ polarized steady-state emission spectra obtained at room temperature for different concentrations. The emission lines correspond to the transitions $^3P_0 \rightarrow {}^3H_{4,5,6}$, $^3P_0 \rightarrow {}^3F_{2,3,4}$ and $^1D_2 \rightarrow {}^3H_{4,5}$. The emission lines are inhomogeneously broadened, which is probably due to the disorder of cations K^+, Bi^{3+}, and rare earth [1] and/or to the existence of several crystallographic sites which could occur if the crystal symmetry is lower than $R\bar{3}m$. This point will be further discussed in the next section. Simultaneous emissions from the transitions $^1D_2 \rightarrow {}^3H_4$ and $^3P_0 \rightarrow {}^3H_6$ are observed in the region between 600 and 630 nm. This was further confirmed by the time-resolved emission spectra and lifetime measurements. At low concentration ($x=0.005$), the most intense emission corresponds to the $^1D_2 \rightarrow {}^3H_4$ transition; however, as concentration rises, the $^1D_2$ emission shows a strong quenching.

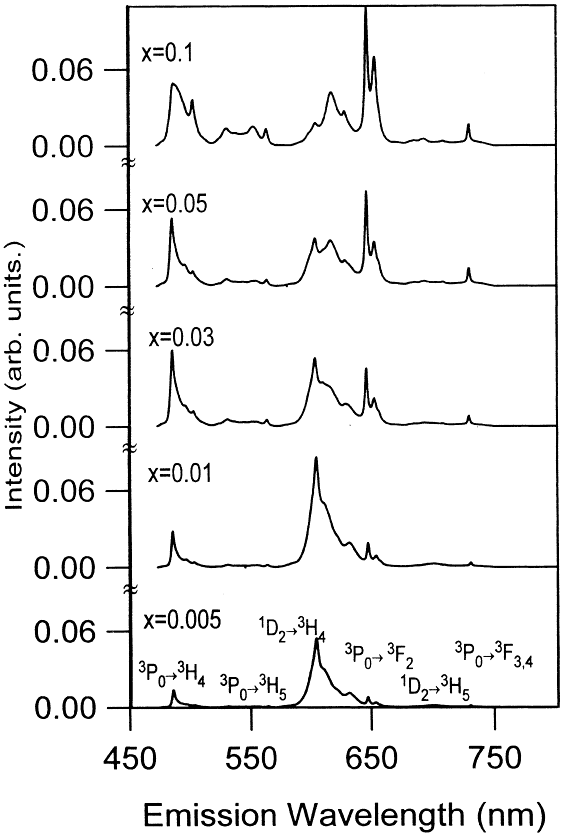

Fig. 1. σ polarized steady-state emission spectra of $K_5Bi_{1-x}Pr_x(MoO_4)_4$ crystal for different Pr^{3+} concentrations obtained at room temperature under 454 nm excitation.

The fluorescence dynamics of the $^3P_0$ and $^1D_2$ emitting levels were investigated as a function of Pr^{3+} concentration. Decay curves for all samples were obtained under laser pulsed excitation at 486 nm, and luminescence was collected at different emission wavelengths between 490 and 720 nm. The $^3P_0$ fluorescence can be described by an exponential function for all concentrations and temperatures. The lifetime values are nearly independent of concentration up to $x=0.1$ at 4.2 and 77 K. Table 1 shows the lifetime values of $^3P_0$ and $^1D_2$ levels at three different temperatures: 4.2, 77 and 295 K. The decays of the $^1D_2$ level can be described at low concentration ($x=0.005$) by an exponential function in the 4.2–295 K temperature range. However, as can be seen in Table 1, as concentration rises the lifetime decreases even at 4.2 K, which indicates that Pr–Pr relaxation processes are present at concentrations higher than $x=0.005$.

Concentration quenching of fluorescence leading to a rapid decrease of the lifetime at high concentration can be due to one or both of the following processes: (i) cross relaxation between Pr^{3+} ions, (ii) migration of the excitation energy due to resonance energy transfer among Pr^{3+} ions and finally (iii) to a quencher center. Energy migration has been described either as a diffusion process or as a random walk (hopping model) [6]. In the case of diffusion-limited decay [6] with dipole–dipole interaction, at long times after the excitation pulse, the fluorescence of the donors decays exponentially with a time constant given by:

$$\frac{1}{\tau} = \frac{1}{\tau_0} + VC_A C_D \qquad (1)$$

Table 1
Lifetimes (μs) of the $^3P_0$ and $^1D_2$ levels as a function of Pr^{3+} concentration at three different temperatures

x	$^3P_0$			$^1D_2$		
	4.2 K	77 K	295 K	4.2 K	77 K	295 K
0.005	3.65	3.6	3.6	87	88	86
0.01	3.61	3.6	3.59	51	50	50
0.03	3.51	3.58	3.55	25	27	26
0.05	3.52	3.52	3.5	12.6	12.2	12.4
0.1	3.55	3.4	3	4.7	4.6	4.1

where V is a constant involving donor–donor and donor–acceptor transfer constants, and C_A and C_D are the acceptor and donor concentrations, respectively. The intrinsic decay time τ_0 is obtained from the low temperature decay of the less concentrated sample, which is purely exponential. In our case we do observe a linear dependence of the effective decay rates with the square of the Pr^{3+} concentration. Therefore, in this concentration range, the linear behaviour shown by the effective decay rates indicates the presence of a dipole–dipole energy transfer process in the framework of a limited-diffusion regime. Under the assumption of electrostatic multipole interaction the donor decay curves can be described by the expression [7]:

$$I(t) = I(0)\exp\left\{-\frac{t}{\tau_0} - \Gamma\left(1-\frac{3}{s}\right)\frac{4}{3}\pi R_0^3 N\left(\frac{t}{\tau_0}\right)^{3/s} - Wt\right\} \tag{2}$$

with $s=6$, 8, and 10, respectively, for electric dipole–dipole, dipole–quadrupole, and quadrupole–quadrupole interactions. N is the donor concentration, R_0 the critical transfer distance, and W the probability of migration-limited relaxation. Fig. 2 shows a least-square fit of the experimental Pr^{3+} decay at 4.2 K to Eq. (2) for two different Pr^{3+} concentrations. As can be observed, a dipole–dipole transfer mechanism is consistent with the experimental decay intensities.

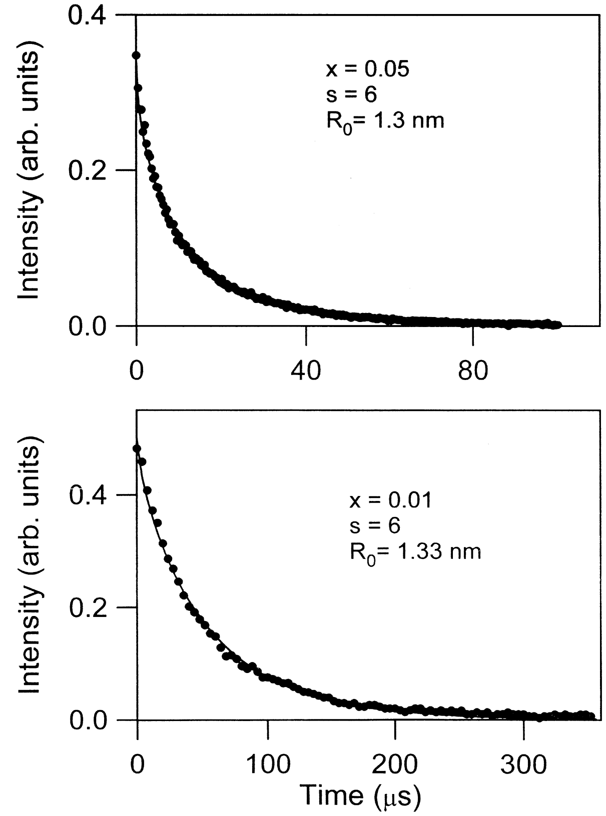

Fig. 2. $^1D_2$ emission of Pr^{3+} showing the fitting between the experimental decay curve (●) and the calculated one (solid line) for: (a) $x=0.05$; (b) $x=0.01$.

An investigation into the inhomogeneous broadening observed in the steady-state and time-resolved emission spectra was performed to obtain information about the possibility of different crystal field sites for Pr^{3+} ions. Although site-selective narrow band excitation within the $^3P_0$ absorption profile was used, the obtained emission spectra of the $^3P_0 \rightarrow {}^3H_4$ transition showed a complex structure, consisting of sharp lines and broad bands which are broader than expected for the instrumental resolution. This indicates a simultaneous excitation of different sets of sites which are probably spectrally overlapped.

3.2. Spectroscopic properties of Eu^{3+}

For a better understanding of the influence of the local coordination on the optical properties of RE ions in these mixed anion crystals we have analyzed the optical properties of Eu^{3+} by making use of laser-induced FLN spectroscopy. Fig. 3 shows the time-resolved fluorescence line-narrowed spectra of the $^5D_0 \rightarrow {}^7F_{0,1,2}$ emissions at 4.2 K obtained under different resonant excitation wavelengths along the $^7F_0 \rightarrow {}^5D_0$ transition, and at 500 μs after the laser pulse in $K_5Bi_{0.95}Eu^{3+}_{0.05}(MoO_4)_4$. As can be observed, the Stark components of the $^7F_1$ multiplet noticeably differ in their evolution with excitation energy. The $^5D_0 \rightarrow {}^7F_1$ transition shows a minimum of three distinct peaks due to the Stark splitting of the $^7F_1$ state, meaning that the Eu^{3+} ions are located in sites with C_{2v} symmetry or lower. The line-narrowed fluorescence of the $^5D_0 \rightarrow {}^7F_2$ hypersensitive transition shows very strong variations as a function of excitation wavelength. A careful analysis of the whole set of spectra makes clear the existence of two principal sites (detected at excitation wavelengths 577.3 and 578.8 nm) for Eu^{3+} with a quite large spectral overlap, and two other additional sites which can be detected only in a very narrow interval of excitation wavelengths (around 579 and 579.9 nm, respectively). At lower concentrations the same behaviour is observed. These results suggest that the influence of the expected statistical disorder among K^+, $(RE)^{3+}$ (or Bi^{3+}) ions in this palmierite-like structure might not be enough to explain the observed features in these spectra. A more plausible approach could be the one considering a lower crystallographic symmetry for the palmierite-like structure of this $K_5Bi_{0.95}Eu^{3+}_{0.05}(MoO_4)_4$ crystal. In a recent work by Lazoryak and Efremov [2], the authors propose a monoclinic P2/m crystal structure for the full concentrated $K_5Nd(MoO_4)_4$ crystal which is attributed to a disorder of the oxygen atoms. For the proposed model, four types of neodymium polyhedra are realized with point symmetries C_2 and C_{2h}, respectively. Two of them have an environment with six oxygen atoms, whereas the other two are embedded in an eight-oxygen polyhedrom. Taking into account that $K_5(RE)(MoO_4)_4$ crystals have in principle a similar crystallographic struc-

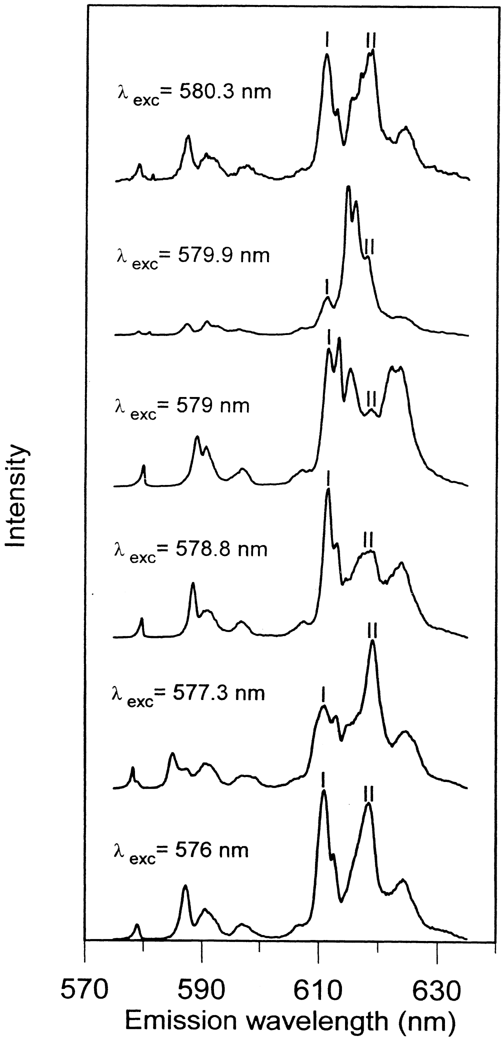

Fig. 3. Time-resolved line-narrowed emission spectra of $^5D_0 \rightarrow {}^7F_{0,1,2}$ transitions of europium ions in $K_5Bi_{0.95}Eu^{3+}_{0.05}(MoO_4)_4$. The fluorescence was measured at 4.2 K at a time delay of 500 μs after the laser pulse and at different excitation wavelengths. Labels (I) and (II) correspond to the two principal sites, respectively.

ture and that, as stated by Klevtsov et al. [4], the statistical distribution of K, Bi, and RE ions make the experimental accuracy insufficient to discuss the details of the structure, we think that our experimental findings confirm the existence (even at low RE concentrations) of low symmetry sites for the rare earth in these palmierite-type crystals.

3.3. Time-resolved $^4F_{3/2} \rightarrow {}^4I_{9/2}$ emission of Nd^{3+}

For Nd^{3+}-doped crystals, site effects were also found in the time-resolved $^4F_{3/2} \rightarrow {}^4I_{9/2}$ emission spectra obtained by exciting the $^4I_{9/2} \rightarrow {}^4G_{5/2}$ hypersensitive transition. In this case, as in the case of Pr^{3+}, the inhomogeneous broadening together with the spectral overlapping of different Stark components impedes a better resolution of the possible sites. Nevertheless, as can be seen in Fig. 4, as time evolves the emission spectrum narrows and smoothly shifts to the red indicating the presence of a broad distribution of Nd^{3+} sites.

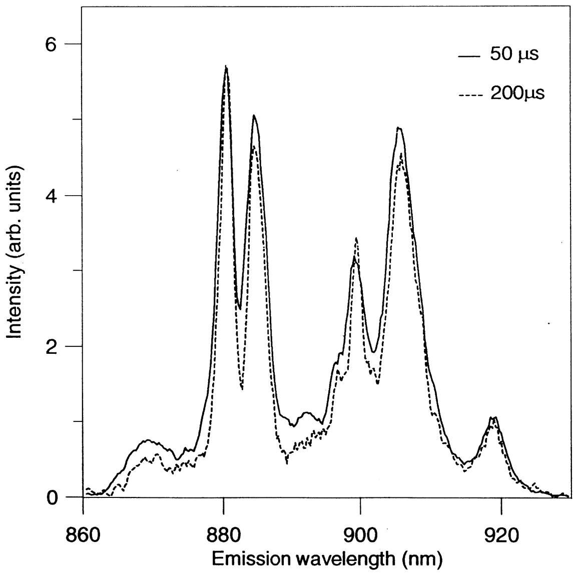

Fig. 4. Time-resolved $^4F_{3/2} \rightarrow {}^4I_{9/2}$ emission spectra obtained by exciting the $^4I_{9/2} \rightarrow {}^4G_{5/2}$ hypersensitive transition in $K_5Bi_{0.95}Nd^{3+}_{0.05}(MoO_4)_4$. The fluorescence was measured at 77 K.

4. Conclusions

(i) Very high optical quality crystals of composition $K_5Bi_{1-x}(RE)_x(MoO_4)_4$, RE=$Pr^{3+}$, Eu^{3+}, Nd^{3+} with $x \leq 0.1$ have been grown.

(ii) For Pr^{3+}-doped crystals, under excitation in the $^3P_0$ state, the crystals show emission from both $^3P_0$ and $^1D_2$ levels.

(iii) Fluorescence quenching of the $^1D_2$ state has been demonstrated to occur for Pr^{3+} concentrations higher than $x=0.005$ even at 4.2 K. A dipole–dipole energy transfer mechanism in the framework of a diffusion-limited relaxation is consistent with the experimental decay intensities.

(iv) Time-resolved fluorescence line-narrowed spectra of the $^5D_0 \rightarrow {}^7F_{0,1,2}$ emissions of Eu^{3+} confirm the existence (even at low Eu^{3+} concentrations) of at least four different low symmetry sites for the rare earth in these palmierite-type crystals.

Acknowledgements

This work has been supported by the Ministerio de Educaciôn y Ciencia (PB95-0512), by the Basque Country Government (PI88/95), and by the Basque Country University (EB034-95).

References

[1] A.A. Kaminskii, S.E. Sarkisov, J. Bohm, P. Reiche, D. Schultze, R. Uecker, Phys. Stat. Sol. 43 (1977) 71.
[2] B.I. Lazoryak, V.A. Efremov, Sov. Phys. Crystallogr. 31 (1986) 138.
[3] G. Huber, W. Lenth, J. Lieberts, F. Lutz, J. Luminesc. 16 (1978) 353.
[4] P.W. Klevtsov, L.P. Kozeeva, V.I. Protasova, L.Yu. Kharchenko, L.A. Glinskaya, R.F. Klevtsova, V.V. Bakakin, Sov. Phys. Crystallogr. 20 (1975) 31.
[5] M.J. Elejalde, R. Balda, J. Fernández, E. Macho, J.L. Adam, Phys. Rev. B 46 (1992) 5169.
[6] M.J. Weber, Phys. Rev. B 4 (1971) 2932.
[7] D.L. Dexter, J. Chem. Phys. 21 (1953) 836.